Potential Formalisms in Electromagnetic-Field Analysis

Natalia K. Georgieva, *Member, IEEE,* and Helen W. Tam

***Abstract*—The theory of electromagnetic (EM) potentials is as old as the Maxwell equations, which treat the field vectors E and H directly. Yet the vector and scalar potentials are often regarded as nothing more than an auxiliary mathematical concept, which does not necessarily reflect a physically existing phenomenon. This widely accepted opinion does not have sound theoretical or experimental validation. The EM potentials are as "real" as the field vectors—they describe observable phenomena and play a crucial role in the explanation of light-matter interactions, radiation, and propagation. We discuss the methodological value of the potential formalism in electromagnetism and the advantages of the potential-based computational approaches in EM analysis. The key points of the discussion are supported by examples of the analysis of classical problems such as the radiation from a small dipole and the field propagation in waveguide structures: a waveguide bend and an H-plane filter. These examples include animations of the propagation of the EM-field potentials and the respective field vectors.**

***Index Terms*—Electromagnetic (EM) potentials, EM theory, EM transient analysis.**

I. Motivation and Outline

ELECTROMAGNETISM is a major branch of physics that describes one of the four known fundamental interactions in nature. It permeates a vast variety of both theoretical and applied sciences. Its applications in electrical, electronic, and telecommunications technology are profound and of utmost importance to the modern world. In engineering science, subjects such as engineering electromagnetics, microwave theory and circuits, and antenna theory and design rest entirely on its fundamental laws. The technology these subjects describe represents a remarkable success in harnessing electromagnetic (EM) energy. It is then somewhat puzzling that we are still far from a complete and contradiction-free understanding of the EM phenomena on both macroscopic and quantum level. Moreover, there are two distinct theoretical models in electromagnetism: the description in terms of field vectors and in terms of potential functions. Although these two formalisms are in agreement—at least in the case of macroscopic electromagnetism—there are cases where the applicability of one or the other is severely limited or completely fails. It is, therefore, important to be acquainted reasonably well with both approaches and to be aware of their limitations.

Unfortunately, contemporary EM-based engineering courses provide limited treatment of the topic of EM potentials—often a result of impossible time restrictions. This treatment relates mostly to antenna/scattering problems in isotropic homogeneous media, e.g., [1] and [2].[1] A generalization of the potential formalism to bi-isotropic homogeneous media is given in [3]. In addition, a deeply rooted opinion permeates texts, as well as research papers, which regards the vector potentials as "strictly mathematical tools" [2], "auxiliary functions" [4], "mainly an aid for computing electromagnetic fields" [5], [6], etc. This opinion is hardly justifiable and it diminishes the real significance of the EM potentials. More importantly, it is in contradiction with quantum electrodynamics, which is an inseparable part of electromagnetism.

Here, we discuss aspects of the theory and the applications of the EM vector and scalar potentials. As a motivation to educators in the field, we would like to point out some merits of the methodology offered by the potential approach to EM-field analysis. First, the EM potentials describe the EM field in its entirety—there is no split into magnetic- and electric-field vectors. Second, the potential approach rests on the wave equation, which is widely employed to describe other wave-like phenomena such as those in acoustics or hydrodynamics. Concepts such as polarization, radiation, diffraction, or scattering can be perceived more intuitively through the potentials as they allow analogies with mechanical waves, which are far more tangible to the novice in the field. Third, the relation between the vector potentials and the current sources is straightforward. This is especially helpful in the case of homogeneous media where the orientation of the vector potential is the same as that of the respective current. Fourth, the vector potentials produce the most natural description of the field in terms of TE and TM modes with respect to a chosen axis, e.g., z. As it is well known, a single-component magnetic vector potential $\mathbf{A} = \hat{\mathbf{z}}A_z$ is sufficient to describe a TM_z mode, the same being true for a single-component electric vector potential $\mathbf{F} = \hat{\mathbf{z}}F_z$ and a TE_z mode [1].[2] Such modal decompositions are widely used in microwave engineering. Also, last but not least, for those who are involved in numerical EM analysis, the computational approaches based on the potential formalism can offer superior accuracy and numerical efficiency for a wide class of problems in comparison with field-based techniques.

Manuscript received May 26, 2002.

The authors are with the Department of Electrical and Computer Engineering, McMaster University, Hamilton, ON, Canada L8S 4K1 (e-mail: talia@mcmaster.ca; tamhw@mcmaster.ca).

This paper has supplementary downloadable material available at http://ieeexplore.ieee.org, provided by the authors. This includes eight GIF files that illustrate the propagation of EM sin waves and pulses. This material is 8.39 MB in size.

Digital Object Identifier 10.1109/TMTT.2003.809188

[1]Here, we limit the discussion to high-frequency electromagnetics and do not refer to vector and scalar potentials in electrostatic and magnetostatic problems.

[2]Throughout the paper, vectors are in bold and unit vectors are denoted by a $\hat{}$.

Below, we briefly review the origins and classical formulation of the potential theory of the EM field. We point out its limitations and proceed with a more general potential formalism, which describes lossy nonhomogeneous media.[3] We discuss the relation between EM potentials and the field vectors, the properties of the vector potentials at material interfaces and sources, as well as their boundary conditions. We then describe the construction of solutions in terms of collinear potentials, their limitations, and advantages. Throughout this paper, the analysis is carried out in the time domain and is supported by numerous examples and animations of the vector potentials and corresponding field vectors.

II. Classical Potential Formalism

EM-field representations in terms of vector and scalar potentials emerged together with the representation in terms of the field vectors $\mathbf{E}$, $\mathbf{D}$, $\mathbf{B}$, and $\mathbf{H}$ in what is now known as Maxwell equations. Indeed, Maxwell himself considered the *electrokinetic momentum* $\mathbf{A}$ a fundamental field vector [7].[4] Pointing out that it relates to the electric current density in a way similar to the way the scalar potential ϕ relates to the charge density, he also refers to it as "the vector-potential of the electric current," which is a vector quantity since the current itself is a vector. Today, only a few are aware that in Chapter IX, "General Equations of the Electromagnetic Field" [7], Maxwell defines the *magnetic induction* $\mathbf{B}$ and the *electromotive intensity* $\mathbf{E}$ as the derivatives of the vector potential $\mathbf{A}$ and scalar potential ϕ as follows:

$$\mathbf{B} = \nabla \times \mathbf{A} \tag{1}$$

$$\mathbf{E} = \mathbf{v} \times \mathbf{B} - \partial_t \mathbf{A} - \nabla \phi \tag{2}$$

where $\mathbf{v}$ represents the velocity of the observation point in the reference coordinate system of the sources and ∂_t is the first-order derivative with respect to time.[5] Equation (2) is the well-known Lorentz force equation.

Furthermore, Maxwell introduces the equations, which define the sources of the EM field. The equation

$$\nabla \times \mathbf{H} = \mathbf{J}_e^t = \sigma_e \mathbf{E} + \partial_t \mathbf{D} + \mathbf{J}_e^i \tag{3}$$

shows the source of the *magnetic force* $\mathbf{H}$ and, hence, of $\mathbf{A}$, followed by

$$\nabla \cdot \mathbf{D} = \rho_e \tag{4}$$

which shows the electric charge density ρ_e as the source of the *electric displacement* $\mathbf{D}$ and, hence, of ϕ. In (3), $\mathbf{J}_e^t$ is the total electric current density, which includes the conduction current density $\mathbf{J}_e^c = \sigma_e \mathbf{E}$ (σ_e being the electric conductivity), the displacement current density $\mathbf{J}_e^D = \partial_t \mathbf{D}$, and the impressed (external) current density $\mathbf{J}_e^i$. The equation

$$-\nabla \times \mathbf{E} = \partial_t \mathbf{B} \tag{5}$$

is not even included in the "general equations," as it is an obvious special case of (2) when $\mathbf{v}$ is parallel to $\mathbf{B}$. Maxwell derives expressions for the vector and scalar potentials in terms of their respective sources, the current, and charge densities, in the form of volume integrals [7] and in the form of second-order wave equations [8]. They are valid in a dispersion-free uniform medium, and are now common knowledge.

Since Maxwell, the science of classical electromagnetism has grown immensely. Most notably, the theory has been developed toward the EM-field analysis in complex and composite media where dispersion, nonuniformity, nonlinearity, and anisotropy/bi-anisotropy are taken into account. What is now known as the Maxwell "curl" equations

$$\begin{aligned} \nabla \times \mathbf{H} &= \partial_t \mathbf{D} + \mathbf{J}_e^c + \mathbf{J}_e^i \\ -\nabla \times \mathbf{E} &= \partial_t \mathbf{B} + \mathbf{J}_m^c + \mathbf{J}_m^i \end{aligned} \tag{6}$$

has become the preferred formalism in comparison with the potential EM-field description in [7]. In (6), $\mathbf{J}_m^c = \sigma_m \mathbf{H}$, where σ_m is the specific magnetic conductivity; and $\mathbf{J}_m^i$ denotes impressed magnetic current density.[6] These additional current densities render the equations in (6) symmetrical and invariant with respect to dual transformations.[7] The Maxwell "divergence" equations

$$\begin{aligned} \nabla \cdot \mathbf{D} &= \rho_e \\ \nabla \cdot \mathbf{B} &= \rho_m \end{aligned} \tag{7}$$

are now viewed as implied by (6). This is indeed true if the EM sources satisfy the fundamental law of continuity

$$\begin{aligned} \nabla \cdot (\mathbf{J}_e^c + \mathbf{J}_e^i) &= -\partial_t \rho_e \\ \nabla \cdot (\mathbf{J}_m^c + \mathbf{J}_m^i) &= -\partial_t \rho_m \end{aligned} \tag{8}$$

where ρ_m denotes the magnetic charge density.[8] The equations in (6) are not sufficient to provide a solution for the four field vectors $\mathbf{E}$, $\mathbf{D}$, $\mathbf{B}$, and $\mathbf{H}$. They are complemented by the constitutive relations [11]

$$\begin{aligned} \mathbf{D} &= \boldsymbol{D}\{\mathbf{E}, \mathbf{B}\} \\ \mathbf{H} &= \boldsymbol{H}\{\mathbf{E}, \mathbf{B}\} \end{aligned} \tag{9}$$

$$\begin{aligned} \mathbf{J}_e &= \boldsymbol{J}_e\{\mathbf{E}, \mathbf{B}\} \\ \mathbf{J}_m &= \boldsymbol{J}_m\{\mathbf{E}, \mathbf{B}\} \end{aligned} \tag{10}$$

[3]The terms *homogeneous* and *nonhomogeneous* are used interchangeably with the terms *uniform* and *nonuniform*, respectively, when describing the properties of the medium.

[4]To avoid confusion, only standard symbols for all EM quantities are used instead of the symbols used in [7].

[5]To make notations concise, partial derivatives are denoted by a ∂. The order of the derivative becomes apparent from the number of variables involved in the differentiation. These variables appear as subscripts.

[6]The magnetic current density is considered a fictitious vector quantity. It is useful in applications based on the equivalence theorem [1]. The specific magnetic conductivity σ_m is an important parameter of fictitious absorbing media known in computational electromagnetics as perfectly matched layers [9].

[7]The concept of duality in electromagnetism is well explained and summarized in [1] and [2].

[8]The magnetic charge density ρ_m is another "unusual" magnetic source, which is considered fictitious since there is no experimental evidence for the existence of magnetic monopoles. It is worth noting, however, that there are strong theoretical arguments [10]–[12] in support of their existence.

where the operators $\boldsymbol{D}$, $\boldsymbol{H}$, $\boldsymbol{J}_e$, and $\boldsymbol{J}_m$ may, in general, be nonlinear operators. For example, for a dispersion-free isotropic and linear, but nonhomogeneous medium, (9) and (10) reduce to

$$\begin{aligned}\mathbf{D}(\mathbf{r}, t) &= \varepsilon(\mathbf{r})\mathbf{E}(\mathbf{r}, t)\\ \mathbf{H}(\mathbf{r}, t) &= \mu^{-1}(\mathbf{r})\mathbf{B}(\mathbf{r}, t)\end{aligned} \tag{11}$$

$$\begin{aligned}\mathbf{J}_e(\mathbf{r}, t) &= \sigma_e(\mathbf{r})\mathbf{E}(\mathbf{r}, t)\\ \mathbf{J}_m(\mathbf{r}, t) &= \sigma_m(\mathbf{r})\mu^{-1}(\mathbf{r})\mathbf{B}(\mathbf{r}, t)\end{aligned} \tag{12}$$

where ε is the dielectric permittivity and μ is the magnetic permeability. Notice that while the field vectors are functions of position $\mathbf{r}$ and time t, the constitutive parameters are functions of position only. Such constitutive relations imply instantaneous response of the medium and are thus an approximation of its interaction with the EM field. It is worth noting that, for a medium to be causal (i.e., it responds after it is stimulated), the time-dependent constitutive relations $\mathbf{D}(\mathbf{E})$ and $\mathbf{B}(\mathbf{H})$ must appear as convolution-type integrals of time [13], [14]. The relations (11) and (12) are acceptable when the medium is nearly dispersion free in a broad frequency band.

The alternative field theory based on potential formulations has seen significant developments as well. In quantum physics, the potentials $\mathbf{A}$ and ϕ are regarded as the "real" field rather than the field vectors $\mathbf{E}$ and $\mathbf{B}$ (or $\mathbf{D}$, $\mathbf{H}$). This is mostly due to the fact that the EM potentials describe properly the interaction between the EM field and charged particles in quantum electrodynamics [15], [16]. The most well-known experimental justification of these concepts is given by the famous Aharonov-Bohm effect [17]. It demonstrates interaction between an electron beam and the EM field in space where the field vectors are zero, but the magnetic vector potential is not. An exceptionally clear description of this experiment and the physical meaning of the EM potentials can be found in [18]. The physical meaning and the "measurability" of $\mathbf{A}$ and ϕ are also examined in [19], [20] where the discussion is based on general physical principles such as the equation of motion and the Lagrangian description of an EM system, and does not require specific knowledge of quantum electrodynamics. Alternative ways to describe the EM power flow and energy in terms of $\mathbf{A}$ and ϕ are considered in [21]–[23].

On the other hand, high-frequency computational electromagnetics is dominated by the field analysis based on (6), (9), and (10) or on the respective second-order vector wave equation for $\mathbf{E}$ or $\mathbf{H}$. This is largely due to the limited applicability of the classical potential formalism based on $(\mathbf{A}, \phi)$ to general problems involving various types of materials and sources. Some examples of the limitations of the classical potential formalism are as follows.

1) It does not allow magnetic sources since (1) implies $\rho_m = 0$ and, therefore, $\mathbf{J}_m = 0$. In that sense, it is incomplete and inconsistent with EM duality unless complemented by dual quantities: the electric vector potential $\mathbf{F}$ and the magnetic scalar potential ψ.
2) In the time domain, it cannot handle nonuniform media exhibiting magnetic losses. This becomes obvious by taking the divergence of the second equation in (6). If the relation (1) is true, then from (6), it follows that (σ_m/μ) is constant in space, i.e., $\nabla(\sigma_m/\mu) = 0$. This is a significant restriction on the generality of the formalism although it involves a fictitious parameter such as σ_m.
3) It does not accommodate dispersive constitutive relations in the time-domain analysis.

In brief, the potential formalism based on $(\mathbf{A}, \phi)$ has been applied to a limited class of high-frequency problems mostly concerning EM-field propagation in vacuum, e.g., antenna and scattering problems. The development of a general potential formalism that can accommodate the vast variety of field–matter interactions remains a challenge both in the frequency- and time-domain analyses.

III. Potentials and Fields

It would be impossible to present here the immense amount of work related to EM potentials. We would rather highlight and illustrate only a few topics from the general vector potential formalism, which serve as a starting point toward more advanced developments such as the *scalar potential techniques* in electromagnetism [24]–[26].[9] The choice of these topics and the way they are presented inevitably reflects a personal viewpoint, and no claim is made with regard to thoroughness and completeness. The intention of this tutorial is to follow a pragmatic and illustrative presentation, which could hopefully clarify the physics behind the potential representation of the EM field. The emphasis is on concepts that could be useful in EM computations and education. We carry out the analysis in the time domain assuming a dispersion-free medium in order to make the discussion more transparent and compatible with the illustrative EM-field animations.

The principle of radiation states that the acceleration (or deceleration) of charges generates a wave-like EM disturbance in space–time [27]. The acceleration of charges is equivalent to time-varying current distributions. We assume the existence of both magnetic and electric current densities $\mathbf{J}_e$ and $\mathbf{J}_m$, which generate their respective vector potentials $\mathbf{A}_\mu$ and $\mathbf{F}_\varepsilon$. In a homogeneous isotropic lossy dielectric-magnetic medium, $\mathbf{A}_\mu$ and $\mathbf{F}_\varepsilon$ satisfy the equations (written in the time-dependent *d'Alambert* form) [28]

$$\begin{aligned}\left(\nabla^2 - \mathcal{T}_{\mu\varepsilon}\right)\mathbf{A}_\mu &= -\mathbf{J}_e\\ \left(\nabla^2 - \mathcal{T}_{\mu\varepsilon}\right)\mathbf{F}_\varepsilon &= -\mathbf{J}_m.\end{aligned} \tag{13}$$

Here, the second-order differential operator in time $\mathcal{T}_{\mu\varepsilon}$ is derived from the first-order operators

$$\begin{aligned}\mathcal{T}_\varepsilon &= \varepsilon\partial_t + \sigma_e\\ \mathcal{T}_\mu &= \mu\partial_t + \sigma_m\end{aligned} \tag{14}$$

as

$$\mathcal{T}_{\mu\varepsilon} = \mathcal{T}_\mu\mathcal{T}_\varepsilon = \mu\varepsilon\partial_{tt} + (\varepsilon\sigma_m + \mu\sigma_e)\partial_t + \sigma_e\sigma_m. \tag{15}$$

[9]The scalar potential techniques study the possibility of EM-field representations in terms of two scalar functions instead of the six-component field-based vectorial formalism. They originated some hundred years ago when Whittaker (1904) [26] proved that only two scalar functions are sufficient to describe the EM field due to any (moving) charge distributions in vacuum.

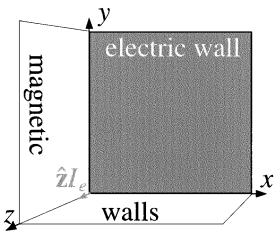

Fig. 1. Computational volume of the dipole radiating in open space.

The operator $\nabla^2 - \mathcal{T}_{\mu\varepsilon}$ defaults to the well-known wave operator $\nabla^2 - \mu\varepsilon\partial_{tt}$ in a loss-free medium. Notice that $\mathbf{A}_\mu$ and $\mathbf{F}_\varepsilon$ relate to the "ordinary" vector potentials as

$$\begin{aligned} \mathbf{A}_\mu &= \mu^{-1}\mathbf{A} \\ \mathbf{F}_\varepsilon &= \varepsilon^{-1}\mathbf{F}. \end{aligned} \tag{16}$$

As a first example, let us consider the EM field in vacuum of a very small dipole (electric current element) whose density we set as $\mathbf{J}_e = \hat{\mathbf{z}} J_{ez}$ in the x–0–y-plane. According to the first equation in (13), a spherical $\mathbf{A}_\mu = \hat{\mathbf{z}} A_{\mu z}$ wave is generated in open space. We examine this wave when the current source is a sinusoidal function of time.

We simulate numerically this problem using a finite-difference algorithm based on the time-domain wave-potential (TDWP) approach [28], which solves the equations in (13) for specified boundary conditions and medium. The computational volume (see Fig. 1) includes only one octant of space because of the symmetry of the problem. There is an electric wall at $z = 0$ and magnetic walls at $x = 0$ and $y = 0$. The remaining three boundaries employ absorbing boundary conditions to simulate reflection-free propagation. The algorithm computes normalized potentials $\mathbf{a} = \sqrt{Z_0}\,\mathbf{A}_\mu$ and $\mathbf{f} = \mathbf{F}_\varepsilon/\sqrt{Z_0}$, both measured in $W^{1/2}$. Here, $Z_0 = \sqrt{\mu_0/\varepsilon_0}$ is the intrinsic impedance of vacuum.

In the z-oriented dipole example, a single-component normalized potential $\mathbf{a} = \hat{\mathbf{z}} a_z$ is computed and a cross section of the wave in the x–0–y-plane is animated in Animation 1.1.[10] In all examples considered in this paper, the computational space is discretized into a uniform mesh. For the current example, we choose a spatial step size $\triangle h = \lambda/30$, where λ is the wavelength in free space corresponding to the frequency of the excitation current ($\lambda = 1$ m). The x- and y-axes in the animation are scaled in terms of the spatial step $\triangle h$. For example, the point $(30,\ 45)$ has actual coordinates $x = 30\triangle h$, $y = 45\triangle h$ with respect to the source point. In terms of wavelengths, these coordinates translate into $x = \lambda$, $y = 1.5\lambda$. We should perhaps also mention that our "small" current source is as small as the mesh allows it to be, i.e., the current element is $I\vec{l} = J_z \triangle h^2 (\hat{\mathbf{z}} \triangle h)$.

In the animation, the spherical symmetry of the a_z wave is well observed. One can also see the decay $\sim 1/r$ of the potential magnitude as the wave moves away from the source. Since the source has small, but finite dimensions, as discussed above, the value of a_z at the source location $(0,\ 0)$ swings between large, but finite values.

[10]All animations hereafter are obtained with in-house software based on the TDWP algorithm [28] unless stated otherwise.

The field components can be computed from the vector potentials if necessary. In this example, we use the relation

$$\mathbf{H} = \nabla \times \mathbf{A}_\mu = -\hat{\varphi}\partial_r A_{\mu z} \tag{17}$$

to compute the H_φ field component (see Animation 1.2). The H_φ wave moving away from the dipole has the same wavelength as the potential wave, of course; however, the slope of the envelope is steeper, i.e., the magnitude of the wave decays more rapidly. This is due to the fact that the $\mathbf{H}$ vector is obtained as a spatial derivative of $\mathbf{A}_\mu$. Generally, the vector potentials are smoother functions in the vicinity of sources and at discontinuities compared to the field vectors. For a short dipole, the amplitude of a potential depends on the distance r from the source as $1/r$, while the terms of the field vectors are proportional to $1/r^n$, where $n = 1, 2, 3$ [27].

One can also compute the electric field vector $\mathbf{E}$ using

$$\mathcal{T}_\varepsilon \mathbf{E} = -\mathcal{T}_{\mu\varepsilon}\mathbf{A}_\mu - \nabla\nabla\cdot\mathbf{A}_\mu. \tag{18}$$

The E_θ-field time-dependent distribution in the x–0–z-plane is shown in Animation 1.3. E_θ is the most significant electric field component far from the source. It is well seen that the far-zone field of the dipole has maximum strength in the x–0–y-plane (azimuthal) and is zero along the dipole's axis, which coincides with the z-axis.

An advantage of the modified vector potentials $\mathbf{A}_\mu$ and $\mathbf{F}_\varepsilon$ is that their sources are exactly the electric and magnetic current densities, respectively; unlike the source terms in the wave equations for the field vectors, which appear as the derivatives of the actual current densities. Thus, in a homogeneous medium, the orientation of $\mathbf{A}_\mu$ and $\mathbf{F}_\varepsilon$ is the same as the orientation of the currents generating them.

When the EM wave propagates in a nonuniform medium, the equations in (13) acquire additional terms [28], [29][11]

$$\begin{aligned} \nabla^2\mathbf{A}_\mu - \mathcal{T}_{\mu\varepsilon}\mathbf{A}_\mu &= -\mathbf{J}_e - (\nabla\mathcal{T}_\varepsilon)\,\Phi - (\nabla\mathcal{T}_\varepsilon)\times\mathbf{F}_\varepsilon \\ \nabla^2\mathbf{F}_\varepsilon - \mathcal{T}_{\mu\varepsilon}\mathbf{F}_\varepsilon &= -\mathbf{J}_m - (\nabla\mathcal{T}_\mu)\,\Psi + (\nabla\mathcal{T}_\mu)\times\mathbf{A}_\mu \end{aligned} \tag{19}$$

where the scalar potentials Φ and Ψ relate to $\mathbf{A}_\mu$ and $\mathbf{F}_\varepsilon$ via the generalized Lorenz gauge

$$\begin{aligned} -\mathcal{T}_\varepsilon\Phi &= \nabla\cdot\mathbf{A}_\mu \\ -\mathcal{T}_\mu\Psi &= \nabla\cdot\mathbf{F}_\varepsilon. \end{aligned} \tag{20}$$

The vector operators $(\nabla\mathcal{T}_\varepsilon)$ and $(\nabla\mathcal{T}_\mu)$ are the gradients of the operators defined in (14) as follows:

$$\begin{aligned} (\nabla\mathcal{T}_\varepsilon) &= (\nabla\varepsilon)\partial_t + (\nabla\sigma_e) \\ (\nabla\mathcal{T}_\mu) &= (\nabla\mu)\partial_t + (\nabla\sigma_m) \end{aligned} \tag{21}$$

so that, e.g.,

$$\begin{aligned} (\nabla\mathcal{T}_\varepsilon)\,\Phi &= (\nabla\varepsilon)\partial_t\Phi + (\nabla\sigma_e)\Phi \\ (\nabla\mathcal{T}_\varepsilon)\times\mathbf{F}_\varepsilon &= (\nabla\varepsilon)\times\partial_t\mathbf{F}_\varepsilon + (\nabla\sigma_e)\times\mathbf{F}_\varepsilon. \end{aligned} \tag{22}$$

The validity of (19) and (20) is not immediately obvious; therefore, it is worthwhile showing that the Maxwell equations

[11]The frequency-domain vector potential analysis of nonhomogeneous media is considered in [30].

follow from them in a rather straightforward manner. Using standard vector identities, (19) can be rewritten as

$$\begin{aligned}&\nabla\times(\nabla\times\mathbf{A}_\mu-\mathcal{T}_\varepsilon\mathbf{F}_\varepsilon-\nabla\Psi)\\&\quad+\mathcal{T}_\varepsilon(\nabla\times\mathbf{F}_\varepsilon+\mathcal{T}_\mu\mathbf{A}_\mu+\nabla\Phi)=\mathbf{J}_e\\&\nabla\times(\nabla\times\mathbf{F}_\varepsilon+\mathcal{T}_\mu\mathbf{A}_\mu+\nabla\Phi)\\&\quad-\mathcal{T}_\mu(\nabla\times\mathbf{A}_\mu-\mathcal{T}_\varepsilon\mathbf{F}_\varepsilon-\nabla\Psi)=\mathbf{J}_m.\end{aligned}\tag{23}$$

The above equations are, in fact, the Maxwell equations

$$\begin{aligned}\nabla\times\mathbf{H}&=\mathcal{T}_\varepsilon\mathbf{E}+\mathbf{J}_e\\-\nabla\times\mathbf{E}&=\mathcal{T}_\mu\mathbf{H}+\mathbf{J}_m\end{aligned}\tag{24}$$

provided that the field vectors are defined according to

$$\begin{aligned}\mathbf{E}&=-\mathcal{T}_\mu\mathbf{A}_\mu-\nabla\Phi-\nabla\times\mathbf{F}_\varepsilon\\\mathbf{H}&=-\mathcal{T}_\varepsilon\mathbf{F}_\varepsilon-\nabla\Psi+\nabla\times\mathbf{A}_\mu.\end{aligned}\tag{25}$$

An alternative potential-to-field relation can be derived by the substitution of (25) into (24) as follows:

$$\begin{aligned}\mathcal{T}_\varepsilon\mathbf{E}&=\nabla\times(\nabla\times\mathbf{A}_\mu-\mathcal{T}_\varepsilon\mathbf{F}_\varepsilon)-\mathbf{J}_e\\\mathcal{T}_\mu\mathbf{H}&=\nabla\times(\nabla\times\mathbf{F}_\varepsilon+\mathcal{T}_\mu\mathbf{A}_\mu)-\mathbf{J}_m.\end{aligned}\tag{26}$$

Once the vector potentials are known, the field vectors can be computed via (25) or (26) if so desired. The information provided by the vector potentials is sufficient for most antenna parameters such as far-field patterns or antenna gain. When the generalized S-parameters [32] are needed, the incident power has to be evaluated at the cross section of each port by integrating over the Poynting vector $\mathbf{S}=\mathbf{E}\times\mathbf{H}$. The respective field components then have to be computed from the potentials at the port locations.

The equations in (19) and (20) are the essence of a recently developed vector potential formalism [28]–[30], which, unlike previous vector potentials models, can handle nonhomogeneous lossy dielectric-magnetic media in the frequency- and time-domain analyses. An attractive feature of this formalism is the transparent relation between the modified vector potentials on one hand and the EM sources on the other. The additional terms due to the medium's nonuniformity show in a straightforward way how coupling occurs between the vector-potential components. Since each vector potential component corresponds to an EM-field mode, one can now estimate the coupling between modes occurring at material interfaces and edges. This is important when estimating the accuracy of "reduced" computational approaches (e.g., [33] and [34]) applied to the analysis of predominantly layered structures where additional modes are excited (but neglected) at material interfaces orthogonal to the major layers.

The additional terms in the right-hand side of (19) can be viewed as sources generating additional disturbances, which distort the field distribution from what it is in a uniform medium. These sources are *implicit* in the sense that they are due to the field's interaction with the medium, unlike the impressed sources, which are explicitly defined (independent of the field) functions of space–time. Let us return to the example of a small dipole. Here is how the inclusion of a layer of dielectric ($\varepsilon_r=4$, $\sigma_e=0$) orthogonal to $\hat{\mathbf{z}}$ leads to a complicated pattern of the $A_{\mu z}$ potential distribution in the elevation plane (see Animation 2). The geometry setup is shown in Fig. 2. The mesh size is the same as in the previous example. The dielectric–air interface is at $z=30\Delta h$. The excitation is now a Gaussian function of time in order to see better the reflection from the dielectric interface and the formation of a guided wave. The pulse duration is 9 ns. This problem can still be analyzed in terms of a single potential $A_{\mu z}$ because the electric current density is parallel to $\hat{\mathbf{z}}$, as is also the gradient of the dielectric permittivity $\nabla\varepsilon=\hat{\mathbf{z}}\partial_x\varepsilon$. Equations (19) suggest that no other vector potential components are generated since the implicit source has only a $\hat{\mathbf{z}}$-component

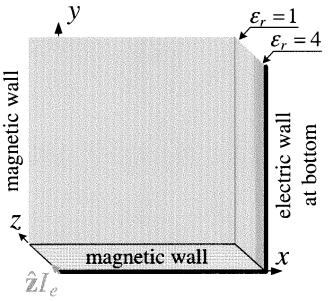

Fig. 2. Computational volume of the dipole buried in a dielectric layer.

$$(\nabla\mathcal{T}_\varepsilon)\,\Phi=-\hat{\mathbf{z}}\varepsilon^{-1}(\partial_z\varepsilon)(\partial_z A_{\mu z}).\tag{27}$$

The equations in (19) are modified for best performance with a finite-difference discretization in nonuniform media [28]; however, the details of the implementation are outside of the scope of this discussion. It is worth noting that all vector potential components are continuous functions at locally flat material interfaces (even in the presence of surface current densities).[12] This is in contrast with the field vector components and is another case in which the smoother distribution of the EM potentials in space becomes obvious.

In microwave and millimeter-wave technology, closed metallic boundaries and inclusions such as vias, strips, waveguide septa and posts, etc., are often encountered. It is, therefore, worthwhile to discuss the boundary conditions for the vector potentials at least in the case of perfectly conducting electric and magnetic walls. The derivation of the boundary conditions for the vector potentials [35] is somewhat confusing for anyone who attempts to solve problems involving, for example, metallic objects. The boundary conditions are viewed as the main reason why the vector potential concept is not particularly popular in the high-frequency EM computational community. One could argue that material interfaces introduce nonuniqueness of the solution in terms of potentials although it does not affect the field vectors [20]. The nonuniqueness of the vector potential boundary conditions is best explained using the transformations of *source equivalence* [29]. They show that EM sources are subject to equivalent transformations that preserve the field intact.

[12]By integrating the equations in (19) over a vanishingly thin interface region, all boundary conditions for the vector potential components and their derivatives along the interface unit normal can be obtained.

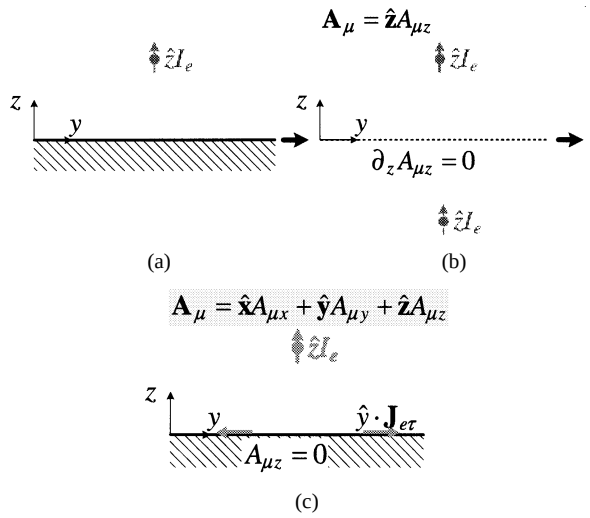

Fig. 3. Dipole above a ground plane: two possible boundary conditions.

Let us examine the simple example considered by Mayergoyz [20] of a dipole above an infinite perfectly conducting metallic plate [see Fig. 3(a)]. According to the equation for $\mathbf{A}_\mu$ in (13), only an $A_{\mu z}$ potential is excited by the dipole. The vanishing tangential electric-field components, expressed according to the Lorenz gauge (20) and the relations in (25), dictate that

$$\begin{aligned} \mathcal{T}_\varepsilon E_x &= \partial_x(\partial_z A_{\mu z}) = 0 \\ \mathcal{T}_\varepsilon E_y &= \partial_y(\partial_z A_{\mu z}) = 0. \end{aligned} \tag{28}$$

An obvious choice of the boundary condition for $A_{\mu z}$ is

$$\partial_z A_{\mu z} = 0. \tag{29}$$

In fact, such a boundary condition sets the electric scalar potential to zero since $\mathcal{T}_\varepsilon \phi = -\partial_z A_{\mu z} = 0$ according to (20). This corresponds to the equivalent problem defined through the method of images [see Fig. 3(b)]. Thus, the problem is entirely defined in terms of a single scalar, the magnetic vector potential component $A_{\mu z}$, governed by the wave equation (13). The space–time distribution of $A_{\mu z}$ generated by an infinitesimal dipole some distance away from a ground plane at $z = 0$ can be seen in Animation 3, where the current source is again a Gaussian function of time. The $A_{\mu z}$ potential distribution is animated in the x–0–z (elevation) plane. The reflection from the ground plane is well observed. Two distinct pulses are formed—the original one and the reflected one—the reflected one following closely behind the original pulse. The vanishing first derivative of $A_{\mu z}$ (29) causes the typical "plateau" shape of the wave at the ground plane $(z = 0)$.

In reality, however, there is no field behind the electric wall and thus $A_{\mu z}$ should be set equal to zero in the conducting region 1 [see Fig. 3(c)]. Consequently, there are surface currents $\mathbf{J}_{e\tau}\delta z = (\hat{\mathbf{x}} J_{ex} + \hat{\mathbf{y}} J_{ey})\delta z$ induced at the perfect conductor's surface layer of infinitesimal thickness δz. According to (26), if the tangential $\mathbf{E}$ components vanish, $\mathbf{J}_{e\tau}$ is not zero and relates to $A_{\mu z}$ as

$$\mathbf{J}_{e\tau} = \hat{\mathbf{x}} \partial_{xz} A_{\mu z} + \hat{\mathbf{y}} \partial_{yz} A_{\mu z}, \qquad \text{at } z = 0. \tag{30}$$

Bearing in mind the relation between currents and vector potentials, we conclude that these currents generate the x and y components of a magnetic vector potential, and those should be included in the computations accordingly. This approach is feasible, and the same field will be obtained, this time, however, at the expense of computing two additional scalar quantities at each point of space–time. It can be shown that this is unnecessary because the tangential surface currents above are equivalent to a planar distribution of normal to the ground electric current density $\mathbf{J}_e^e = \hat{\mathbf{z}} J_{ez}^e$, which implies the boundary condition (29) for the homogeneous[13] wave equation of $A_{\mu z}$. According to the theory of source equivalence [29], the field generated by the current density defined in (30) is equivalent to the field generated by

$$\hat{\mathbf{z}} J_{ez}^e = \hat{\mathbf{z}}(\partial_z \mathcal{P}_e + \mathcal{T}_\varepsilon \mathcal{E}_z) \tag{31}$$

where

$$\begin{aligned} \nabla_\perp^2 \mathcal{P}_e &= -\nabla_\perp \cdot \mathbf{J}_{e\tau} \\ \nabla_\perp^2 \mathcal{E}_z &= \nabla_\perp \times \mathbf{J}_{e\tau}. \end{aligned} \tag{32}$$

In (32), $\nabla_\perp = \hat{\mathbf{x}}\partial_x + \hat{\mathbf{y}}\partial_y$, and $\nabla_\perp^2$ is the two-dimensional (2-D) Laplace operator $\nabla_\perp^2 = \partial_{xx} + \partial_{yy}$. From (30) and (32), it follows that

$$\mathcal{E}_z = 0, \quad \mathcal{P}_e = -\partial_z A_{\mu z}, \qquad \text{at } z = 0. \tag{33}$$

The functions $\mathcal{E}_z$ and $\mathcal{P}_e$ are identically zero everywhere else since $\mathbf{J}_{e\tau}$ exists only at $z = 0$. If we now integrate the wave equation for $A_{\mu z}$ with the equivalent sources (31) at the vanishingly thin surface layer δz

$$\begin{aligned} \partial_z A_{\mu z} + \int_{\delta z} (\nabla_\perp^2 - \mathcal{T}_{\mu\varepsilon}) A_{\mu z}\, dz \\ = -\int_{\delta z} J_{ez}^e\, dz = -J_{ez_s}^e = -\mathcal{P}_e \end{aligned} \tag{34}$$

and let $\delta z \to 0$, we obtain

$$\partial_z A_{\mu z} + \mathcal{P}_e = 0, \qquad \text{at } z = 0 \tag{35}$$

since $\mathcal{P}_e = -\partial_z A_{\mu z}$. The above relation shows that the equivalent surface layer of $\hat{\mathbf{z}}$-directed current density compensates the $\partial_z A_{\mu z}$ derivative, which is nonzero because of the assumption of vanishing $A_{\mu z}$ in the conducting region. Thus, in effect, the current distribution $J_{ez_s}^e$ makes the solution equivalent to a homogeneous wave equation for $A_{\mu z}$ with a homogeneous Neumann boundary condition (29) at $z = 0$.

In general, the simplest—although not the only possible—boundary conditions for the vector potentials at electric and magnetic walls can be obtained from (25) in a homogeneous Dirichlet or Neumann form by setting the respective tangential field components equal to zero. Thus, at an electric wall of unit normal $\hat{\mathbf{n}}$, they appear as

$$\begin{aligned} \partial_n(\hat{\mathbf{n}} \cdot \mathbf{A}_\mu) &= 0 \\ \hat{\mathbf{n}} \times \mathbf{A}_\mu &= 0 \\ \hat{\mathbf{n}} \cdot \mathbf{F}_\varepsilon &= 0 \\ \partial_n(\hat{\mathbf{n}} \times \mathbf{F}_\varepsilon) &= 0. \end{aligned} \tag{36}$$

[13]The term *homogeneous* here refers to the wave equation (not the medium) and emphasizes that its source term is zero.

a	17.4244
b	15.7988
δ	0.62230
W_1	13.0683
W_2	11.8237
W_3	11.2014
W_4	11.2014
L_1	16.1798
L_2	16.1798
L_3	16.8021
all dimensions in mm	

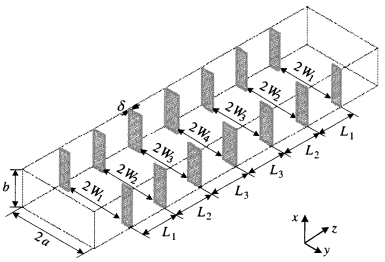

Fig. 4. Geometry and dimensions of the H-plane waveguide filter.

The boundary conditions at magnetic walls are obtained by duality. It can also be shown [28] that when a vector potential component is parallel to an edge along $\hat{\boldsymbol{\tau}}$, its boundary conditions still appear in the above simple form; e.g., for a metallic edge

$$\hat{\boldsymbol{\tau}} \cdot \mathbf{A}_\mu = 0. \tag{37}$$

IV. Solutions in Terms of Pairs of Collinear Potentials

The above discussion on the treatment of material interfaces in the vector potential formalism is essential in understanding the modal behavior of the field and construction of an efficient solution in terms of potential functions instead of the field vectors. For example, in a stratified medium where the constitutive parameters depend on a single coordinate along the axis $\hat{\mathbf{n}}$ normal to the layers, the solution can be carried out in terms of a single-component magnetic vector potential $\mathbf{A}_\mu = \hat{\mathbf{n}} A_{\mu n}$, as it was done in the second example of a dipole buried in a dielectric layer. This analysis yields a solution in terms of the TM_n mode.[14] Note that the TM_n mode is analyzed independently of the TE_n mode (corresponding to $\mathbf{F}_\varepsilon = \hat{\mathbf{n}} F_{\varepsilon n}$ and excited by $\mathbf{J}_m = \hat{\mathbf{n}} J_{mn}$) as both modes are decoupled according to (19). Of course, the orientation of the vector potential depends also on its impressed sources, which may have components transversal to $\hat{\mathbf{n}}$. However, such components can be transformed into $\hat{\mathbf{n}}$-directed electric and/or magnetic current densities using the equivalent source transformations [29]. This can be done offline (outside of the actual field computation) as the impressed current densities are explicitly defined functions of space–time.

In a similar manner, if all edges in the volume of interest are of the same orientation, the most efficient analysis is in terms of the vector potential which is: i) parallel to the edges and ii) corresponds to the desired mode. Consider the H-plane waveguide filter in Fig. 4. There are $\hat{\mathbf{x}}$-directed edges in this structure which leaves us a choice between $\mathbf{A}_\mu = \hat{\mathbf{x}} A_{\mu x}$ and $\mathbf{F}_\varepsilon = \hat{\mathbf{x}} F_{\varepsilon x}$. If the structure is to be analyzed for the dominant TE_{z01} mode then the $A_{\mu x}$ potential is the proper choice ($\mathbf{F}_\varepsilon = \hat{\mathbf{x}} F_{\varepsilon x} = \mathbf{0}$ for waveguide modes independent of x). Animation 4.1 shows the propagation of a band-limited (5–10 GHz) EM pulse in terms of the $A_{\mu x}$ potential through the filter. We simulate matched waveguide ports at both ends of the filter using absorbing boundary conditions. The $A_{\mu x}$ is set to zero at the edges of the septa according to (37). This makes the locations of the septa along the guide well visible in the animation. The boundary conditions at the waveguide walls are $A_{\mu x} = 0$ at $y = 0$ and $y = 2a$, and $\partial_x A_{\mu x} = 0$ at $x = 0$ and $x = b$. The discretization mesh is uniform with a step size $\Delta h = \delta$, where δ is the septum thickness (see Fig. 4). As before, the axes are scaled in terms of Δh. The reflection coefficient and insertion loss of the filter are plotted in Fig. 5. They are computed from the time-domain waveforms of the $A_{\mu x}$ potential recorded at the input and output waveguide ports. For verification, the S-parameters generated by a commercial finite-element solver (Agilent HFSS[15]) are plotted as well.

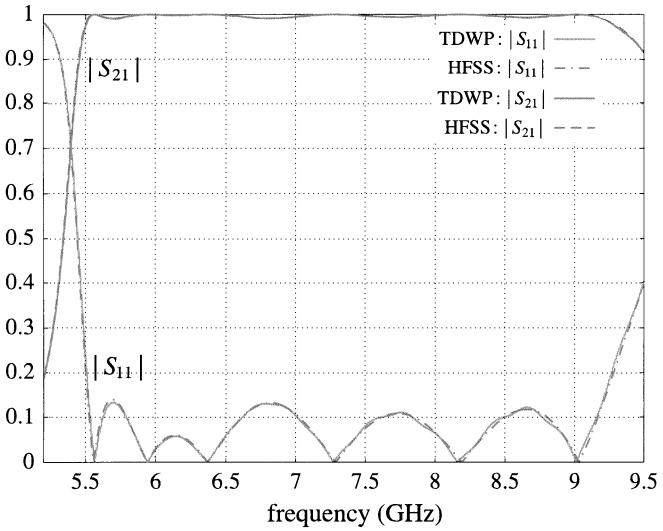

Fig. 5. Magnitudes of the S-parameters of the H-plane waveguide filter.

In summary, in a region of the computational volume where: 1) the gradients of the constitutive parameters (if not zero) are parallel to the direction specified by $\hat{\mathbf{n}}$; 2) the conducting edges (if present) are along $\hat{\mathbf{n}}$; and 3) all sources have been transformed into $\hat{\mathbf{n}}$-oriented current densities, *any* field mode can be described using *one* of the two potential components $A_{\mu n}$ or $F_{\varepsilon n}$. The field representation is thus reduced (or *scalarized*) to two decoupled modes, the TM_n and the TE_n mode, which can be analyzed separately.[16] Such regions are said to have a distinguished axis $\hat{\mathbf{n}}$. An obvious special case is the open space where any axis can be chosen as distinguished unless specified by the orientation of a radiating source. The computational advantages of using a potential approach to the analysis of such regions are obvious. In a finite-difference implementation, solving a single wave equation instead of the Maxwell equations leads to a threefold reduction in both CPU time and memory requirements.

To avoid any confusion with currently existing TE/TM decomposition techniques in computational electromagnetics, it is worthwhile discussing their applicability and the difference from the potential approach. When the field does not depend on one of the spatial coordinates, a 2-D field solver can perform the analysis with a reduced computational effort. In the 2-D case, the Maxwell equations decouple into two groups of equations: a TE and TM field, where the TE/TM decomposition is with respect to the *axis of field invariance* [9], e.g., $\hat{\mathbf{x}}$ in the case of the TE_{z01} mode in the waveguide filter example.

[14]Here, the term *mode* refers only to the orientation of the respective vector potential and is in no way descriptive of the field distribution in the plane transverse to $\hat{\mathbf{n}}$.

[15]*HFSS, ver. 5.5*, Agilent Technologies, Santa Rosa, CA, 1999.

[16]The procedure is also referred to as *TE/TM field decomposition* [1], [2]. It is widely used in the construction of Green's functions for stratified media, as well as the solution to waveguide and radiation problems.

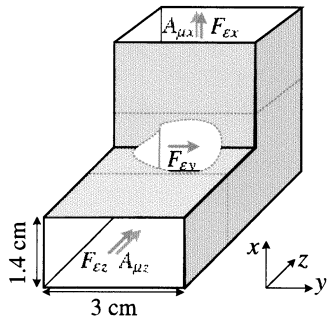

Fig. 6. Geometry of the E-plane waveguide bend. The TE_{z01} mode is excited through the $F_{\varepsilon y}$ potential component, but the reflected and transmitted waves contain higher order modes.

Each of these modes requires the computation of three scalars. For example, the TM_x mode of an x-independent field involves the E_x, H_y, and H_z components. Due to the reduction of the computational volume to a 2-D plane and the reduction of the number of unknown scalars computed at each point from six to three, the 2-D field-based computations are significantly faster than their three-dimensional (3-D) full-wave counterparts. To illustrate this technique, the dominant mode of the H-plane waveguide filter is simulated again, this time with the 2-D solver MEFiSTo-2D Classic[17] which is based on the transmission-line matrix (TLM) method. Either one of the three computed field components, i.e., E_x, H_y or H_z, can be observed. Animation 4.2 shows the EM wave in terms of the E_x component. Notice that in the case of the dominant TE_{z01} mode, $\partial_x A_{\mu x} = 0$. Thus, $E_x = -\mu_0 \partial_t A_{\mu x}$ according to (25). The spatial distribution of E_x is, therefore, very similar to that of $A_{\mu x}$. This is well seen from both animations Animation 4.1 and Animation 4.2.

It must be emphasized that the 2-D field-based analysis is very different from the potential-based analysis. In the former, the TE mode decouples from the TM mode due to the field invariance along one of the axis, thereby limiting its applicability to 2-D problems. In the latter, the TE mode decouples from the TM mode due to the specific properties of the regions of distinguished axis $\hat{\mathbf{n}}$, thereby providing a *full-wave* solution in terms of two decoupled modes, i.e., the TM_n mode described by $A_{\mu n}$ and the TE_n mode described by $F_{\varepsilon n}$.

Take as an example, the E-plane waveguide bend shown in Fig. 6. This is a 3-D problem regardless of the mode we analyze it for. It still can be solved in terms of a single-component vector potential ($F_{\varepsilon y}$ or $A_{\mu y}$) as it contains only one edge along the y-axis. Mode equivalence [28] shows that the dominant TE_{z01} mode is represented by $F_{\varepsilon y}$ ($A_{\mu y} = 0$). The $F_{\varepsilon y}$ potential is excited with a limited bandwidth from 5 to 10 GHz to suppress higher order modes in the transient response. The EM wave is shown in Animation 5 in terms of $F_{\varepsilon y}$ in the x–0–z-plane (the E-plane). The animation illustrates the normalized potential $f_y = F_{\varepsilon y}/\sqrt{Z_0}$, $W^{1/2}$. The vertical electric-field component corresponding to the dominant mode is calculated at each port and is used to obtain the S-parameters (see Fig. 7).

The incident field pulse is excited so that it is independent of the vertical coordinate x at the input waveguide section, which corresponds to the dominant-mode field distribution. However, the E-plane bend introduces higher order modes

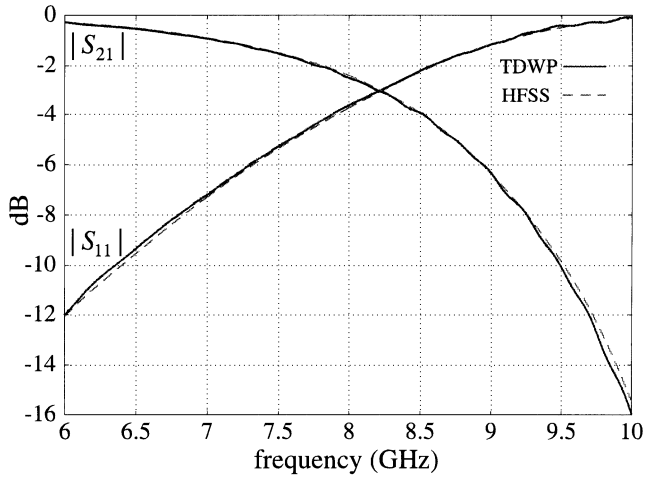

Fig. 7. Magnitudes of the S-parameters of the E-plane waveguide bend.

in the reflected wave, which now depends on x, as well as in the transmitted wave, which now depends on z. This is well seen in Animation 5, where, initially, the incident wave is independent of the x-coordinate. After the reflection, the total field is obviously dependent on x, which indicates the presence of higher order modes. The same effect is observable in the transmitted wave as well. It is seen that it depends on z, especially in the region close to the bend. Depending on the excited frequencies and the dimensions of the waveguide cross section, the higher order "content" may be of propagating and/or evanescent modes. In this particular example, the cross section of the waveguide is such that higher order modes are evanescent. They quickly decay as the observation point moves away from the bend, i.e., the wave becomes less and less dependent on the vertical coordinate (e.g., x in the input guide).

V. Conclusion

We now have a clear understanding of the conditions that allow the field representation in terms of two decoupled modes. These are the conditions defining a region of distinguished axis $\hat{\mathbf{n}}$. They impose significant restrictions on the problems solvable in terms of a single-component vector potential. It is, therefore, important to answer the questions: 1) is it possible to generalize the scalar potential representation to problems of practical importance, e.g., involving arbitrarily oriented gradients of the constitutive parameters and perfectly conducting edges and 2) at what expense?[18] The answer to the first question is positive. The price one has to pay is that the two modes represented by the scalar wave potentials $A_{\mu n}$ and $F_{\varepsilon n}$ are coupled so that they cannot be analyzed separately anymore. In computational terms, it means that two second-order wave equations are solved simultaneously. In a finite-difference algorithm, this amounts to two-thirds of the computational requirements of a field-based vectorial algorithm such as the finite-difference time-domain (FDTD) method. The coupling can be accounted for by domain subdivision of the computational volume and equivalent modal transformations [28]. Other possibilities arise from the source equivalence theory [29]. Potential-based solutions using finite-differences exhibit excellent accuracy even with coarse grids,

[17]*MEFiSTo-2D Classic*, Faustus Sci. Corporation, Victoria, BC, Canada [Online]. Available: http://www.faustcorp.com

[18]The discussion can be extended into the realm of anisotropic and bi-anisotropic media, but this reaches far beyond the goals of this tutorial.

which is due to their smooth distribution in the vicinity of interfaces, edges, and sources.

The application of the scalar potential techniques to a variety of problems arising in high-frequency electronics and in photonics is an exciting and novel venue of research. Thus far, the research on the EM potentials in electrodynamics has been largely confined to theoretical developments and discussions. The purpose of this tutorial would be achieved if it succeeds in encouraging interest in the subject of EM potentials and its development toward useful applications and computational approaches.[19]

Finally, the theory of EM potentials provides a different perspective into the physics of electromagnetism, a viewpoint which reveals its similarity to other familiar wave phenomena in the physical world. It certainly provides a better intuitive understanding of radiation and wave propagation. Thus, if properly presented, it offers an invaluable methodology for the educators in the field.

REFERENCES

[1] R. F. Harrington, *Time–Harmonic Electromagnetic Fields*. New York: McGraw-Hil, 1961, Classic Textbook Reissue.

[2] C. A. Balanis, *Advanced Engineering Electromagnetics*. New York: Wiley, 1989.

[3] I. V. Lindell, *Methods for Electromagnetic Field Analysis*. Piscataway, NJ: IEEE Press, 1992.

[4] R. E. Collin, *Field Theory of Guided Waves*, 2nd ed. Piscataway, NJ: IEEE Press, 1991.

[5] P. Hammond, "The role of the potentials in electromagnetism," *Int. J. Comput. Math. Elect. Electron. Eng.*, vol. 18, no. 2, pp. 103–119, 1999.

[6] I. V. Lindell and F. Olyslager, "Potentials in bi-anisotropic media," *J. Electromagn. Waves Applicat.*, vol. 15, pp. 3–18, 2001.

[7] J. C. Maxwell, *A Treatise on Electricity & Magnetism*. New York: Dover, 1954, vol. 2, ch. IX, pp. 247–259.

[8] ——, *A Treatise on Electricity & Magnetism*. New York: Dover, 1954, vol. 2, ch. XX, pp. 431–438.

[9] A. Taflove, *Computational Electrodynamics: The Finite-Difference Time-Domain Method*. Boston, MA: Artech House, 1995.

[10] P. A. M. Dirac, "Quantized singularities in the electromagnetic field," in *Proc. R. Soc. Lond. A, Math. Phys. Sci.*, vol. A133, 1931, pp. 60–72.

[11] J. D. Jackson, *Classical Electrodynamics*, 3rd ed. New York: Wiley, 1998, pp. 273–280.

[12] G. Lochak, "The symmetry between electricity and magnetism and the problem of the existence of a magnetic monopole," in *Advanced Electromagnetism: Foundations, Theory and Applications*, T. W. Barrett and D. M. Grimes, Eds. Singapore: World Scientific, 1995.

[13] J. D. Jackson, *Classical Electrodynamics*, 3rd ed. New York: Wiley, 1998, pp. 13–16.

[14] W. S. Weiglhofer and A. Lakhtakia, "On causality requirements for material media," *Arch. Elektron. Uebertrag.*, vol. 50, no. 6, pp. 389–391, 1996.

[15] R. P. Feynman, R. B. Leighton, and M. Sands, *The Feynman Lectures on Physics*. Reading, MA: Addison-Wesley, 1964, vol. 2, pp. 15–22.

[16] ——, *QED: The Strange Theory of Light and Matter*. Princeton, NJ: Princeton Univ. Press, 1985.

[17] Y. Aharonov and D. Bohm, "Significance of electromagnetic potentials in the quantum theory," *Phys. Rev.*, vol. 115, pp. 485–491, Aug. 1959.

[18] F. Gronwald and J. Nitsch, "The structure of the electromagnetic field as derived from first principles," *IEEE Antennas Propagat. Mag.*, vol. 43, pp. 64–79, Aug. 2001.

[19] E. J. Konopinski, "What the electromagnetic vector potential describes," *Amer. J. Phys.*, vol. 46, no. 5, pp. 499–502, May 1978.

[20] I. D. Mayergoyz, "Some remarks concerning electromagnetic potentials," *IEEE Trans. Magn.*, vol. 29, pp. 1301–1305, Mar. 1993.

[21] C. J. Carpenter, "Electromagnetic energy and power in terms of charges and potentials instead of the fields," *Proc. Inst. Elect. Eng.*, pt. A, vol. 136, no. 2, pp. 55–65, Mar. 1989.

[22] ——, "Comparison of the practical advantages of alternative descriptions of electromagnetic momentum," *Proc. Inst. Elect. Eng.*, pt. A, vol. 136, no. 3, pp. 101–114, May 1989.

[19]It should be noted that EM potentials are already widely used in computations of electrostatic and magnetostatic nature.

[23] ——, "Teaching electromagnetism in terms of the potentials instead of the 'Maxwell' equations," *IEEE Trans. Educ.*, vol. 36, no. 2, pp. 223–226, May 1993.

[24] A. Nisbet, "Electromagnetic potentials in a heterogeneous nonconducting medium," in *Proc. R. Soc. Lond. A, Math. Phys. Sci.*, vol. 240, 1957, pp. 375–381.

[25] W. S. Weiglhofer, "Scalar Hertz potentials for linear bianisotropic mediums," in *Electromagnetic Fields in Unconventional Materials and Structures*, O. N. Singh and A. Lakhtakia, Eds. New York: Wiley, 2000, pp. 1–37.

[26] E. Whittaker, *A History of the Theories of Aether & Electricity*. New York: Harper & Brothers, 1960 (reprint), vol. 1, pp. 409–410.

[27] C. A. Balanis, *Antenna Theory: Analysis and Design*. New York: Wiley, 1997.

[28] N. K. Georgieva, "Construction of solutions to electromagnetic problems in terms of two collinear vector potentials," *IEEE Trans. Microwave Theory Tech.*, vol. 50, pp. 1950–1959, Aug. 2002.

[29] N. K. Georgieva and W. S. Weiglhofer, "Electromagnetic vector potentials and the scalarization of sources in a nonhomogeneous medium," *Phys. Rev. E, Stat. Phys. Plasmas Fluids Relat. Interdiscip. Top.*, vol. 66, Oct. 2002.

[30] W. S. Weiglhofer and N. K. Georgieva, "Vector potentials and scalarization for nonhomogeneous isotropic mediums," *Electromagnetics*, to be published.

[31] N. K. Georgieva and W. S. Weiglhofer, "Electromagnetic vector potentials in isotropic nonhomogeneous materials: mode equivalence and scalarization," *Proc. Inst. Elect. Electron. Eng.*, pt. H, to be published.

[32] D. K. Misra, *Radio-Frequency and Microwave Communication Circuits*. New York: Wiley, 2001.

[33] W.-P. Huang, S. T. Chu, A. Goss, and S. K. Chaudhuri, "A scalar finite-difference time-domain approach to guided-wave optics," *IEEE Photon. Technol. Lett.*, vol. 3, pp. 524–526, June 1991.

[34] W.-P. Huang, S. T. Chu, and S. K. Chaudhuri, "A semi-vectorial finite-difference time-domain method," *IEEE Photon. Technol. Lett.*, vol. 3, pp. 803–806, Sept. 1991.

[35] N. Georgieva and E. Yamashita, "Time-domain vector-potential analysis of transmission-line problems," *IEEE Trans. Microwave Theory Tech.*, vol. 46, pp. 404–410, Apr. 1998.

[36] G. Matthaei, L. Young, and E. M. T. Jones, *Microwave Filters, Impedance-Matching Networks, and Coupling Structures*. Norwood, MA: Artech House, 1980, p. 545.

Natalia K. Georgieva (S'93–M'97) received the Ph.D. degree from the University of Electro-Communications, Tokyo, Japan, in 1997.

From 1998 to 1999, she was with the Natural Sciences and Engineering Research Council of Canada (NSERC), during which time she was initially with the Microwave and Electromagnetics Laboratory, DalTech, Dalhousie University, Halifax, NS, Canada. For a year, she was then with the Simulation Optimization Systems Research Laboratory, McMaster University, Hamilton, ON, Canada. In July 1999, she joined the Department of Electrical and Computer Engineering, McMaster University, where she is currently an Assistant Professor. Her research interests include theoretical and computational electromagnetism, high-frequency analysis techniques, as well as computer-aided design (CAD) methods for high-frequency structures and antennas.

Dr. Georgieva was the recipient of an NSERC Post-Doctoral Fellowship from 1998 to 1999. She currently holds the 2000 NSERC University Faculty Award.

Helen W. Tam received the B.Sc. degree in electrical and computer engineering from the University of Toronto, Toronto, ON, Canada, in 1999, and the M.A.Sc. degree in electrical and computer engineering from McMaster University, Hamilton, ON, Canada, in 2002.

Her interests include electromagnetics-based design sensitivity analysis and time-domain computational methods.